Supplementary Information for

Systematic RNA interference reveals that oncogenic *KRAS*-driven cancers require TBK1

David A. Barbie, Pablo Tamayo, Jesse S. Boehm, So Young Kim, Susan E. Moody, Ian F. Dunn, Anna C. Schinzel, Peter Sandy, Etienne Meylan, Claudia Scholl, Stefan Frohling, Edmond M. Chan, Martin L. Sos, Kathrin Michel, Craig Mermel, Serena J. Silver, Barbara A. Weir, Jan H. Reiling, Qing Sheng, Piyush B. Gupta, Raymond C. Wadlow, Hanh Le, Sebastian Hoersch, Ben S. Wittner, Sridhar Ramaswamy, David M. Livingston, David M. Sabatini, Matthew Meyerson, Roman K. Thomas, Eric S. Lander, Jill P. Mesirov, David E. Root, D. Gary Gilliland, Tyler Jacks, William C. Hahn*

*To whom correspondence should be addressed. Email: william_hahn@dfci.harvard.edu

This file includes:

Figure legends for Supplementary Figures 1 through 11

Supplementary Tables 1 through 5

Supplemental Figures 1 through 11

Figure Legends

Supplementary Fig. 1. Schematic of experimental design. Large scale shRNA screens for proliferation/viability were performed in 19 cell lines using a library of 5002 shRNAs targeting 957 genes enriched in kinases and phosphatases. Cancer cell lines harboring oncogenic *KRAS* alleles were identified and segregated from cell lines with wild type (WT) *KRAS* alleles. Complementary computational approaches were utilized to identify genes whose suppression selectively impaired proliferation/viability in *KRAS* mutant cells. Candidate genes were then retested in a secondary screen in a new panel of cell lines. *KRAS* itself was the top-ranked gene identified by this approach, followed by *TBK1*.

Supplementary Fig. 2. *KRAS*-specific shRNAs identified by computational analysis of RNAi screening datasets suppress *KRAS* expression. (*a*) Immunoblot of KRAS in DLD-1 cells expressing *KRAS*-specific shRNAs. The three *KRAS* shRNAs that resulted in selective proliferation/viability impairment in *KRAS* mutant cell lines in the primary screens (denoted by *) all efficiently suppressed *KRAS* expression. (*b*) B-score values were averaged for these three *KRAS*-specific shRNAs in each cell line, and compared between *KRAS* wild-type (WT) and *KRAS* mutant cell lines from the primary screens. Dotted line reflects a B-score value of zero. *KRAS* dependence was greater in cell lines carrying *KRAS* mutations than in wild type cells ($p<0.01$, t-test).

Supplementary Fig. 3. *KRAS* mutation status and *KRAS* dependence of non-small cell lung cancer (NSCLC) cell lines selected for the secondary screen. (*a*) *KRAS* codon 12 was sequenced

in all cell lines (3'-5' direction shown), confirming the known *KRAS* mutation status of each line. (*b*) Viability following suppression of *KRAS* expression with 2 different *KRAS*-specific shRNAs across the 4 cell lines with mutant *KRAS* (left) and 4 WT *KRAS* cell lines (right). Cell viability data was determined using CellTiterGlo and correlated with apoptosis (see Supplementary Fig. 4). The mean and standard error of the mean (SEM) of triplicate samples normalized to the effects of the shGFP control vector are shown.

Supplementary Fig. 4. *KRAS* suppression induces apoptosis in cell lines harboring *KRAS* mutations (*a*) Immunoblot of KRAS following *KRAS*-specific shRNA expression across all 8 lung cancer cell lines to confirm target suppression. Lysates were prepared 72 h after expression of the indicated shRNAs. KRAS protein was not observed at baseline in NCI-H522 cells. (*b*) Immunoblot of cleaved PARP in lysates from NCI-H23 cells (mutant *KRAS*) compared with NCI-H1437 cells (wild type *KRAS*) revealed specific induction of PARP cleavage in NCI-H23 cells following *KRAS* suppression. (*c*) Immunoblot of KRAS in NCI-H23 cells expressing additional *KRAS*-specific shRNAs tested in the secondary screen. Lysates were prepared 72 h after expression of the indicated shRNAs.

Supplementary Fig. 5. shRNAs in the secondary screen showed selective proliferation/viability impairment in *KRAS* mutant cells. (*a*) Viability data was normalized using percent of control (POC) and $\log_{10}$ transformed to center values around zero. As described in the full methods, we independently screened this panel of cell lines with two sets of control shRNAs: 20 control shRNAs targeting exogenous reporter genes included on the screening plate, in addition to a separate larger set of 84 control shRNAs, to provide an additional measure of the background

distribution for this secondary screen. Data was analyzed using the t-test statistic in Comparative Marker Selection to identify shRNAs that selectively impaired proliferation/viability in *KRAS* mutant cell lines relative to wild-type cell lines for both the candidate secondary screen plate and the control shRNA plate that was screened independently. The resulting lists of shRNAs were filtered to identify shRNAs with significant viability impairment in the mutant *KRAS* class, defined as class mean LogPOC<-0.2 (~37% viability impairment). A more negative value on the x-axis indicates more selective effects on proliferation/viability in the mutant *KRAS* class. A significantly greater proportion (y-axis) of shRNAs from the secondary screen plate selectively impaired proliferation/viability in *KRAS* mutant cells compared with the control shRNA plate (p=0.0002). We used the t-test statistic threshold that was maximally achieved by the set of control shRNAs (dotted line) as the boundary to identify the top 25 shRNAs *KRAS* synthetic lethal shRNAs that scored on the candidate plate. (*b*) Supervised analysis identified 6 *KRAS*-specific shRNAs (bold) within the top 25 candidate shRNAs that induced selective proliferation/viability impairment in cells harboring mutant *KRAS*. Two out of 5 *TBK1*-specific shRNAs tested (bold) were also identified within this list. Red represents increased proliferation/viability and blue represents decreased proliferation/viability.

Supplementary Fig. 6. *TBK1* suppression induces apoptosis in cells with mutant *KRAS* in a RAF- and AKT-independent manner. (*a*) DAPI (blue) and TUNEL staining (green) of NCI-H23 (upper panels) and NCI-1437 cells (lower panels) 5 d following TBK1 suppression. (*b*) Immunoblot of murine Tbk1 and cleaved caspase 3 in LKR13 cells 72 h following *Tbk1* suppression. The only *Tbk1*–specific shRNA resulting in effective Tbk1 suppression (shTbk1-2222) induced significant cleavage of caspase 3. (*c*) Confirmation of *CRAF*, *BRAF*, *AKT1*, and *RALB* suppression by specific shRNAs. We note that *RALB* shRNAs were not assayed in the

primary shRNA screens. (*d*) Immunoblot of phosho-ERK and phospho-AKT following *KRAS* or *TBK1* suppression (effective *TBK1*-specific shRNAs denoted by *). Suppression of *TBK1* expression in these same lysates is shown in Fig. 2a.

Supplementary Fig. 7. NF-κB target gene activation downstream of oncogenic *KRAS*. (*a*) Shown is the enrichment plot for a RAS oncogenic signature, which was the most significantly correlated gene set with oncogenic *KRAS* expression in AALE cells. Two separate NF-κB gene sets were identified in the top 10 out of 1844 gene sets examined, and a third TNF-related NF-κB signature was identified just below this threshold. Red represents enrichment in AALE-K samples, blue represents enrichment in AALE-V samples, black lines represent individual members of the gene set, and the green plot represents the distribution of enrichment scores. (*b*) Expression of the IKKε regulated NF-κB target genes compared with IRF3 target genes in AALE-K and AALE-V cells (duplicate samples). Red represents up-regulation, blue represents down-regulation. Arrows denote genes examined following TBK1 suppression in (*c*). (*c*) Quantitative RT-PCR was used to analyze the expression of genes from the IRF3 and IKKε-NF-κB subsets in cancer cell lines expressing mutant *KRAS* (NCI-H23) following expression of shRNAs specific for *KRAS*, *TBK1* or GFP. The mean and SD of triplicate experiments normalized to GAPDH as an internal amplification control are shown.

Supplementary Fig. 8. Regulation of IKBα family members by KRAS and TBK1. (*a*) Fractionation of lysates from AALE-K and AALE-V cells was performed to assess the levels of cytoplasmic IKBα and nuclear IRF3. Densitometry was used to normalize IKBα levels to GAPDH (cytoplasmic marker) and nuclear IRF3 levels to lamin A/C (nuclear marker). (*b*) IKBα

and p105 levels were measured using densitometry of immunoblots shown in Fig. 3e and normalized to actin levels. Values were compared with those found in control AALE-V cells.

Supplementary Fig. 9. Inhibition of NF-κB activity selectively impairs viability of isogenic cells expressing oncogenic KRAS. Cell viability measured 6 d after expression of a control vector (pBP) or an IκBα-super-repressor (IKB-SR) in AALE-K or AALE-V cells. Cell viability data represents the mean of triplicate samples normalized to control vector expression. Specific viability impairment was noted following IKB-SR expression in AALE-K cells ($p \leq 0.008$, t-test).

Supplementary Fig. 10. c-REL inhibition induces apoptosis in KRAS mutant and dependent cells (*a*) Immunoblot of IRF3 and c-REL in NCI-H23 cells (mutant *KRAS*) following *IRF3* or *c-REL*-specific shRNA expression. Lysates were prepared 72 h after expression of the indicated shRNAs. PARP cleavage correlated with the degree of c-REL suppression (lower panel, right). (*b*) Nuclear/cytoplasmic fractionation of lysates in cells expressing *TBK1*- or *GFP*-specific shRNAs in NCI-H23 cells. Immunoblotting was performed using antibodies specific for p105, c-REL, and TBK1. (*c*) Specific co-immunoprecipitation of p105, but not TBK1, with endogenous c-REL in NCI-H23 cells. (*d*) Expression of anti-apoptotic genes in NCI-H23 cells following expression of shTBK1 or shGFP by qRT-PCR. Mean and SD of triplicate experiments normalized to GAPDH are shown.

Supplementary Fig. 11. BCL-XL expression fails to rescue viability following *survivin* suppression in *KRAS* mutant cells. (*a*) NCI-H23 cells stably expressing a V5-tagged BCL-XL or a control protein (LACZ) were generated, and cell viability was examined 6 d following

expression of *TBK1*-, *survivin*-, or *GFP*-specific shRNAs. The means and SD of triplicate samples, normalized to the effects of the shGFP control vector are shown. (*b*) Over-expression of V5-tagged BCL-XL and suppression of TBK1 and survivin was confirmed by immunoblotting. Lysates were prepared 72 h after expression of the indicated shRNAs.

Supplementary Table 1
Cell Lines Tested in Primary Screens

Cell Lines	Tissue of Origin	*KRAS* Status
MDA-MB-231	Breast	G13D
HCT116	Colon	G13D
DLD1	Colon	G13D
TOV21G	Ovarian	G12C
A549	Lung	G12S
RPMI-8226	Myeloma	G12A*
NOMO-1	Leukemia	G13D
THP-1	Leukemia	Wild Type
T47D	Breast	Wild Type
MCF7	Breast	Wild Type
MDA-MB-453	Breast	Wild Type
U87	Glioblastoma	Wild Type
LN229	Glioblastoma	Wild Type*
OVCAR8	Ovarian	Wild Type*$^{+}$
PC3	Prostate	Wild Type
LNCaP	Prostate	Wild Type
786-0	Renal	Wild Type*$^{+}$
Normal Human Fibroblasts	Skin	Wild Type
HMEC-TERT	Mammary Epithelium	Wild Type

*Discordance between *KRAS* mutation status and *KRAS* dependence noted in primary screen
$^{+}$RAS/NF-κB signature positive

Supplementary Table 2
Candidate *KRAS* Synthetic Lethal Genes

Hairpin-Level Analysis	Hairpin Set (RIGER) Analysis
ADRBK2	*ADRBK2*
CDC2L1	*ARHGEF2*
CPNE1	*BRCA1*
EPHA6	*CDC2*
FIGN	*CDC2L2*
HSPA5	*CDKN2C*
INSRR	*CLK3*
KRAS	*CNP*
MAP3K11	*DYRK1B*
MAPK9	*EPHA6*
MAPK14	*FIGN*
NME6	*FLT3LG*
RAF1	*FN3KRP*
STK35	*FXN*
TBK1	*GPSM2*
TSSK2	*HSPA5*
VRK3	*INSRR*
	KRAS
	LOC390529
	LOC401313
	LOC402434
	MAP3K8
	MAPK14
	MAPKAP1
	MAPKAPK5
	MASK
	NME6
	NR1I2
	NR1I3
	PPARA
	PRKRA
	PSKH2
	PSMD14
	PTCH2
	STK35
	TBK1
	TSSK2
	VRK1
	VRK3
	YSK4

Supplementary Table 3. Top 250 shRNAs identified by feature selection method

shRNA	Gene	t-test score
NM_005160.x-630s1c1	ADRBK2	-3.91
NM_053006.x-321s1c1	TSSK2	-3.56
NM_016440.x-150s1c1	VRK3	-3.51
NM_003161.x-1417s1c1	RPS6KB1	-3.47
NM_020642.2-413s1c1	C11orf17	-3.46
NM_006875.x-551s1c1	PIM2	-3.38
NM_005430.2-1060s1c1	W01	-3.38
NM_139012.x-503s1c1	MAPK14	-3.38
NM_007181.x-790s1c1	MAP4K1	-3.37
NM_003992.x-301s1c1	CLK3	-3.36
NM_173655.x-424s1c1	EPHA6	-3.34
NM_001699.x-2187s1c1	AXL	-3.21
NM_014683.x-945s1c1	ULK2	-3.20
NM_003682.2-2486s1c1	MADD	-3.19
NM_001222.x-1384s1c1	CAMK2G	-3.16
NM_080789.1-153s1c1	ACPT	-3.14
NM_015247.1-2059s1c1	CYLD	-3.10
NM_145162.x-791s1c1	MAP2K5	-3.03
NM_003845.x-635s1c1	DYRK4	-3.02
NM_173655.x-1500s1c1	EPHA6	-2.96
NM_025052.x-665s1c1	YSK4	-2.96
NM_021976.3-1463s1c1	RXRB	-2.93
NM_005805.1-754s1c1	PSMD14	-2.93
NM_024960.3-703s1c1	PANK2	-2.89
NM_006098.2-388s1c1	GNB2L1	-2.88
NM_017771.x-686s1c1	PXK	-2.88
NM_052827.1-908s1c1	CDK2	-2.87
NM_001799.x-878s1c1	CDK7	-2.86
NM_002082.x-788s1c1	GRK6	-2.85
NM_139069.x-401s1c1	MAPK9	-2.84
NM_006243.2-1800s1c1	PPP2R5A	-2.83
NM_006374.3-485s1c1	STK25	-2.82
NM_007294.1-356s1c1	BRCA1	-2.81
NM_002953.x-957s1c1	RPS6KA1	-2.79
NM_022073.x-692s1c1	EGLN3	-2.75
NM_014705.2-2965s1c1	DOCK4	-2.74
NM_005027.2-1934s1c1	PIK3R2	-2.74
NM_016524.x-716s1c1	SYT17	-2.73
NM_005198.3-686s1c1	CHKB	-2.71
NM_004197.x-1177s1c1	STK19	-2.69
NM_005036.x-495s1c1	PPARA	-2.68
NM_002908.1-2071s1c1	REL	-2.68
NM_016308.1-367s1c1	CMPK	-2.63
NM_001459.2-398s1c1	FLT3LG	-2.62
NM_022158.2-413s1c1	FN3K	-2.62
NM_003384.x-1070s1c1	VRK1	-2.61

NM_016440.x-793s1c1	VRK3	-2.61
NM_005734.x-2302s1c1	HIPK3	-2.59
NM_003738.2-300s1c1	PTCH2	-2.58
NM_003889.2-2805s1c1	NR1I2	-2.58
NM_004760.x-439s1c1	STK17A	-2.55
NM_018086.x-1172s1c1	FIGN	-2.52
NM_007014.x-173s1c1	WWP2	-2.52
NM_033360.2-509s1c1	KRAS	-2.51
NM_000141.x-3402s1c1	FGFR2	-2.50
NM_005347.x-1593s1c1	HSPA5	-2.48
NM_001787.1-2043s1c1	CDC2L1	-2.47
NM_002752.x-160s1c1	MAPK9	-2.46
NM_014215.x-2201s1c1	INSRR	-2.45
NM_004333.2-1106s1c1	BRAF	-2.45
NM_003952.x-1618s1c1	RPS6KB2	-2.44
NM_005104.2-2059s1c1	BRD2	-2.43
NM_080836.x-814s1c1	STK35	-2.42
NM_002513.2-841s1c1	NME3	-2.42
NM_053006.x-268s1c1	TSSK2	-2.40
NM_080836.x-790s1c1	STK35	-2.38
NM_014586.x-1347s1c1	HUNK	-2.38
NM_005793.x-212s1c1	NME6	-2.37
NM_005713.1-1059s1c1	COL4A3BP	-2.37
NM_033126.x-241s1c1	PSKH2	-2.35
NM_004635.3-550s1c1	MAPKAPK3	-2.35
NM_139021.x-284s1c1	MAPK15	-2.35
XM_066534.2-369s1c1	DGKK	-2.35
NM_054113.2-315s1c1	CIB3	-2.34
NM_004723.x-2698s1c1	ARHGEF2	-2.34
NM_003647.1-1829s1c1	DGKE	-2.34
NM_006888.2-461s1c1	CALM1	-2.34
NM_152230.2-1075s1c1	IPMK	-2.34
NM_024779.3-298s1c1	PIP5K2C	-2.33
NM_145203.2-1021s1c1	CSNK1A1L	-2.32
NM_001433.x-3319s1c1	ERN1	-2.31
NM_005160.x-1226s1c1	ADRBK2	-2.31
NM_000222.x-173s1c1	KIT	-2.31
NM_013254.x-1536s1c1	TBK1	-2.30
NM_001315.x-1118s1c1	MAPK14	-2.28
NM_001123.x-991s1c1	ADK	-2.28
NM_015375.1-2638s1c1	RIPK5	-2.28
NM_004327.x-3023s1c1	BCR	-2.27
NM_024960.3-391s1c1	PANK2	-2.27
NM_003236.1-61s1c1	TGFA	-2.27
NM_013296.3-2024s1c1	GPSM2	-2.26
NM_031464.2-1783s1c1	RPS6KL1	-2.26
NM_005356.x-1281s1c1	LCK	-2.25
NM_002945.2-122s1c1	RPA1	-2.25
NM_005456.x-1442s1c1	MAPK8IP1	-2.25

NM_003390.x-3616s1c1	WEE1	-2.24
NM_004131.3-585s1c1	GZMB	-2.24
NM_001786.x-820s1c1	CDC2	-2.24
NM_001259.x-515s1c1	CDK6	-2.23
NM_006282.x-287s1c1	STK4	-2.23
NM_003494.x-6841s1c1	DYSF	-2.23
NM_005983.2-1374s1c1	SKP2	-2.22
NM_001744.x-354s1c1	CAMK4	-2.22
NM_005546.x-430s1c1	ITK	-2.22
NM_024876.2-530s1c1	ADCK4	-2.22
NM_018086.x-855s1c1	FIGN	-2.21
NM_033360.2-407s1c1	KRAS	-2.21
NM_006374.3-1004s1c1	STK25	-2.19
NM_198452.1-352s1c1	PNCK	-2.19
NM_014840.x-1935s1c1	NUAK1	-2.18
NM_002880.x-1764s1c1	RAF1	-2.18
NM_003640.2-4162s1c1	IKBKAP	-2.18
NM_003390.x-1966s1c1	WEE1	-2.18
NM_005255.x-1870s1c1	GAK	-2.18
NM_007174.1-5709s1c1	CIT	-2.17
NM_004714.x-778s1c1	DYRK1B	-2.17
NM_001363.2-760s1c1	DKC1	-2.17
NM_024117.x-1308s1c1	MAPKAP1	-2.14
NM_002576.x-1184s1c1	PAK1	-2.14
NM_006238.x-1314s1c1	PPARD	-2.14
NM_003253.1-3630s1c1	TIAM1	-2.14
NM_014381.1-2936s1c1	MLH3	-2.13
NM_000251.1-441s1c1	MSH2	-2.11
NM_005541.2-2387s1c1	INPP5D	-2.11
NM_004714.x-1353s1c1	DYRK1B	-2.11
NM_006256.1-3041s1c1	PKN2	-2.10
NM_017572.2-565s1c1	MKNK2	-2.10
NM_001346.x-1954s1c1	DGKG	-2.09
NM_033123.x-1864s1c1	PLCZ1	-2.08
NM_153809.1-1464s1c1	TAF1L	-2.08
NM_033133.x-1010s1c1	CNP	-2.07
NM_000144.3-796s1c1	FXN	-2.06
NM_000368.2-3671s1c1	TSC1	-2.05
NM_001203.x-742s1c1	BMPR1B	-2.04
NM_002529.x-214s1c1	0RK1	-2.04
NM_001982.1-2653s1c1	ERBB3	-2.04
NM_021133.x-1216s1c1	RNASEL	-2.04
NM_032037.1-692s1c1	TSSK6	-2.04
NM_020366.x-3819s1c1	RPGRIP1	-2.03
NM_006098.2-297s1c1	GNB2L1	-2.02
NM_005204.x-870s1c1	MAP3K8	-2.02
NM_001203.x-1519s1c1	BMPR1B	-2.02
NM_004517.x-700s1c1	ILK	-2.02
NM_003936.3-1091s1c1	CDK5R2	-2.01

NM_004444.x-459s1c1	EPHB4	-2.01
NM_021158.3-604s1c1	TRIB3	-2.01
NM_199345.1-721s1c1	LOC375133	-2.00
NM_001625.2-764s1c1	AK2	-2.00
NM_002759.x-904s1c1	EIF2AK2	-2.00
NM_005793.x-109s1c1	NME6	-1.99
NM_000551.2-625s1c1	VHL	-1.99
NM_024800.x-1146s1c1	NEK11	-1.99
XM_371835.1-4974s1c1	IBTK	-1.98
NM_005233.3-4735s1c1	EPHA3	-1.98
NM_001743.3-468s1c1	CALM2	-1.98
NM_005122.2-1028s1c1	NR1I3	-1.97
NM_004087.1-832s1c1	DLG1	-1.96
NM_015148.2-905s1c1	PASK	-1.96
NM_019841.x-2249s1c1	TRPV5	-1.96
NM_005307.x-753s1c1	GRK4	-1.96
NM_025144.2-1319s1c1	ALPK1	-1.96
NM_001626.x-656s1c1	AKT2	-1.95
NM_003215.x-1286s1c1	TEC	-1.94
NM_000061.x-1266s1c1	BTK	-1.94
NM_000298.3-1633s1c1	PKLR	-1.94
NM_024594.2-377s1c1	PANK3	-1.93
NM_001982.1-1638s1c1	ERBB3	-1.93
NM_000875.2-1400s1c1	IGF1R	-1.93
NM_002880.x-321s1c1	RAF1	-1.92
NM_014216.3-754s1c1	ITPK1	-1.92
NM_001274.2-1030s1c1	CHEK1	-1.92
NM_022740.x-1389s1c1	HIPK2	-1.91
NM_003668.x-855s1c1	MAPKAPK5	-1.91
NM_001001329.1-408s1c1	PRKCSH	-1.91
NM_152928.1-1652s1c1	CPNE1	-1.90
NM_031914.x-151s1c1	SYT16	-1.89
NM_018127.4-1863s1c1	ELAC2	-1.89
NM_003718.x-3040s1c1	CDC2L5	-1.89
NM_004360.2-2057s1c1	CDH1	-1.89
NM_002929.x-372s1c1	GRK1	-1.89
NM_025259.3-2524s1c1	MSH5	-1.88
NM_006293.x-743s1c1	TYRO3	-1.88
NM_001262.2-1464s1c1	CDKN2C	-1.88
NM_005465.x-1757s1c1	AKT3	-1.87
NM_001211.x-1560s1c1	BUB1B	-1.86
NM_003180.x-1844s1c1	SYT5	-1.86
NM_006712.3-978s1c1	FASTK	-1.85
NM_014365.x-638s1c1	HSPB8	-1.85
NM_013330.x-591s1c1	NME7	-1.85
NM_002419.2-3071s1c1	MAP3K11	-1.85
NM_003503.x-1638s1c1	CDC7	-1.84
NM_000297.2-2005s1c1	PKD2	-1.84
NM_002736.1-612s1c1	PRKAR2B	-1.84

NM_001894.x-462s1c1	CSNK1E	-1.84
NM_013355.x-1240s1c1	PKN3	-1.83
NM_017771.x-1038s1c1	PXK	-1.83
NM_005751.3-2615s1c1	AKAP9	-1.83
NM_005347.x-1285s1c1	HSPA5	-1.83
NM_001259.x-468s1c1	CDK6	-1.83
NM_014326.x-1735s1c1	DAPK2	-1.83
NM_005235.1-1189s1c1	ERBB4	-1.82
NM_004573.x-2070s1c1	PLCB2	-1.82
NM_001616.x-568s1c1	ACVR2A	-1.82
NM_022128.x-932s1c1	RBKS	-1.82
NM_152928.1-1275s1c1	CPNE1	-1.81
NM_002752.x-401s1c1	MAPK9	-1.81
NM_001744.x-501s1c1	CAMK4	-1.81
NM_005923.x-1110s1c1	MAP3K5	-1.81
NM_016231.x-1320s1c1	NLK	-1.80
NM_198291.1-648s1c1	SRC	-1.80
NM_001221.x-1475s1c1	CAMK2D	-1.80
NM_017572.2-1172s1c1	MKNK2	-1.80
NM_020629.x-432s1c1	RET	-1.79
NM_079421.2-376s1c1	CDKN2D	-1.79
NM_007064.x-3696s1c1	KALRN	-1.79
NM_152696.3-796s1c1	HIPK1	-1.79
NM_014215.x-1595s1c1	INSRR	-1.78
NM_001220.x-1340s1c1	CAMK2B	-1.78
NM_005232.2-2341s1c1	EPHA1	-1.78
NM_002447.x-4136s1c1	MST1R	-1.78
NM_005030.3-513s1c1	PLK1	-1.78
NM_001787.1-2259s1c1	CDC2L1	-1.77
NM_001184.2-8099s1c1	ATR	-1.77
NM_000534.x-276s1c1	PMS1	-1.77
NM_006258.x-3498s1c1	PRKG1	-1.77
NM_004336.x-2317s1c1	BUB1	-1.77
XM_031706.8-2907s1c1	MAPKBP1	-1.76
NM_013233.x-737s1c1	STK39	-1.75
NM_001345.4-592s1c1	DGKA	-1.75
NM_013254.x-1212s1c1	TBK1	-1.75
NM_032409.1-1036s1c1	PINK1	-1.75
NM_001274.x-1317s1c1	CHEK1	-1.75
NM_001204.x-1962s1c1	BMPR2	-1.75
NM_001260.x-335s1c1	CDK8	-1.74
NM_003010.2-3471s1c1	MAP2K4	-1.74
NM_002419.2-1501s1c1	MAP3K11	-1.74
NM_017593.x-539s1c1	BMP2K	-1.74
NM_003160.x-1228s1c1	AURKC	-1.74
NM_018216.1-897s1c1	PANK4	-1.74
NM_002591.2-836s1c1	PCK1	-1.73
NM_000076.1-1399s1c1	CDKN1C	-1.73
NM_005028.3-533s1c1	PIP5K2A	-1.72

NM_003656.x-871s1c1	CAMK1	-1.72
NM_004690.x-738s1c1	LATS1	-1.72
NM_144610.x-316s1c1	FLJ25006	-1.72
NM_003690.3-802s1c1	PRKRA	-1.72
NM_006238.x-1932s1c1	PPARD	-1.71
NM_030952.x-454s1c1	NUAK2	-1.71
NM_017726.x-385s1c1	PPP1R14D	-1.71

Supplementary Table 4. Genes identified by RIGER with NES < -1

Gene	NES
EPHA6	-11.1
TBK1	-10.6
TSSK2	-9.97
YSK4	-9.72
FN3KRP	-7.69
ARHGEF2	-7.18
KRAS	-7.07
FIGN	-6.46
NR1I2	-6.23
CDKN2C	-5.9
CDC2	-5.86
FXN	-5.81
GPSM2	-5.76
CLK3	-5.75
HSPA5	-5.4
STK35	-5.15
MAPK14	-4.89
PSMD14	-4.85
LOC401313	-4.59
LOC402434	-4.46
MAPKAP1	-4.43
MST4	-4.06
INSRR	-4.05
PRKRA	-4.02
VRK3	-4.02
CDC2L2	-4.01
NR1I3	-3.95
PTCH2	-3.91
VRK1	-3.82
CNP	-3.67
MAP3K8	-3.64
PSKH2	-3.58
DYRK1B	-3.58
FLT3LG	-3.52
NME6	-3.32
MAPKAPK5	-3.3
ADRBK2	-3.18
BRCA1	-3.17
GRK6	-3.15
PPARA	-3.14
LOC390529	-3.13
PANK2	-3.07
UMP-CMPK	-3.03
RAF1	-3.02
CDH1	-2.99
PXK	-2.83

IGF1R	-2.83
CDK7	-2.69
RPS6KB1	-2.67
ACVR1B	-2.62
ASK	-2.58
AURKB	-2.54
PNCK	-2.49
CSNK1E	-2.48
GK2	-2.46
MAP3K12	-2.44
LOC51760	-2.43
Pparg	-2.34
BMPR1A	-2.32
MAP3K11	-2.3
FGFR2	-2.28
CDKL3	-2.15
PLCB2	-2.12
MPP1	-2.09
SYT14L	-2.08
MUSK	-2.08
FN3K	-2.05
WEE1	-2.05
PKN3	-2.05
CALM2	-1.99
CDC2L1	-1.96
PCTK1	-1.96
MAPK9	-1.94
Gabra2	-1.87
STK4	-1.84
FLJ25006	-1.84
PIK3C2G	-1.83
REL	-1.83
DKFZP434C131	-1.8
SF1	-1.78
CDKN1C	-1.73
MAP2K5	-1.73
MAP4K5	-1.69
LOC441689	-1.68
CDC7	-1.66
PIK3AP1	-1.66
FLJ34389	-1.64
E2F1	-1.61
PIP5K2A	-1.6
ILKAP	-1.6
NTRK2	-1.6
PSKH1	-1.59
LOC139189	-1.59
C17orf31	-1.58
DLG2	-1.57

CAMK2G	-1.55
FLJ21438	-1.53
IBTK	-1.49
DCC	-1.48
LOC253289	-1.43
RPS6KL1	-1.42
DGKG	-1.41
AATK	-1.39
DAPK1	-1.38
Gabra3	-1.38
MAK	-1.37
GAK	-1.37
DCAMKL1	-1.37
CDKN2D	-1.33
BMPR1B	-1.31
PKN1	-1.31
CYLD	-1.27
EXO1	-1.25
PRKDC	-1.25
IRAK2	-1.23
DDR1	-1.23
STK11IP	-1.23
POT1	-1.21
CSNK2B	-1.2
RPS6KA6	-1.2
DLG4	-1.19
PFKFB3	-1.18
STK33	-1.18
CPNE1	-1.17
SSTK	-1.17
PRKCB1	-1.17
MGC4238	-1.15
PI4K2B	-1.15
BCR	-1.14
XRCC5	-1.14
CDK9	-1.14
ACVR1	-1.14
ARK5	-1.14
ERBB3	-1.14
NEK8	-1.11
TGFBR1	-1.1
TRPV6	-1.09
NJMU-R1	-1.08
FLJ40852	-1.08
MKNK2	-1.08
DYRK4	-1.08
LOC392347	-1.07
NME3	-1.02
TTK	-1.01

Supplementary Table 5. Identities of validated shRNAs used in this study

shRNA	TRC Identifier	NM number	Sequence (5'-3')
shKRAS-2	TRCN0000033263	NM_033360.2-269s1c1	GACGAATATGATCCAACAATA
shKRAS-3	TRCN0000033262	NM_033360.2-509s1c1	CCTATGGTCCTAGTAGGAAAT
shKRAS-5	TRCN0000033260	NM_033360.2-407s1c1	GAGGGCTTTCTTTGTGTATTT
shKRAS-6	TRCN0000040151	NM_004985.3-297s1c1	CTACAGGAAGCAAGTAGTAA
shKRAS-7	TRCN0000040152	NM_004985.3-492s1c1	AGGACTCTGAAGATGTACCTA
shKRAS-8	TRCN0000040150	NM_004985.3-570s1c1	CTCAGGACTTAGCAAGAAGTT
shKRAS-9	TRCN0000040149	NM_004985.3-641s1c1	GATGCCTTCTATACATTAGTT
shKRAS-10	TRCN0000010369	NM_004985.x-1160s1c1	CAGTTGAGACCTTCTAATTGG
shKRAS-11	TRCN0000040148	NM_004985.3-3896s1c1	CCTCGTTTCTACACAGAGAAA
shTBK1-1	TRCN0000003182	NM_013254.x-1773s1c1	GCAGAACGTAGATTAGCTTAT
shTBK1-4	TRCN0000003185	NM_013254.x-1536s1c1	GCGGCAGAGTTAGGTGAAATT
shCRAF-1	TRCN0000001066	NM_002880.x-1236s1c1	CGGAGATGTTGCAGTAAAGAT
shCRAF-2	TRCN0000001068	NM_002880.x-1529s1c1	GAGACATGAAATCCAACAATA
shCRAF-3	TRCN0000001065	NM_002880.x-1764s1c1	GCTTCCTTATTCTCACATCAA
shBRAF-1	TRCN0000006289	NM_004333.2-1106s1c1	GCAGATGAAGATCATCGAAAT
shBRAF-2	TRCN0000006290	NM_004333.2-838s1c1	CCGCTGTCAAACATGTGGTTA
shBRAF-3	TRCN0000006292	NM_004333.2-1538s1c1	CAGCAGTTACAAGCCTTCAAA
shAKT1-1	TRCN0000010163	NM_005163.x-642s1c1	CGAGTTTGAGTACCTGAAGCT
shAKT1-2	TRCN0000010174	NM_005163.x-981s1c1	GGACTACCTGCACTCGGAGAA
shAKT1-3	TRCN0000010162	NM_005163.x-1044s1c1	GGACAAGGACGGGCACATTAA
shRALB-1	TRCN0000072957	NM_002881.2-302s1c1	GAGTTTGTAGAAGACTATGAA
shRALB-2	TRCN0000072954	NM_002881.2-419s1c1	GCCATTCGAGATAACTACTTT
shRALB-3	TRCN0000072956	NM_002881.2-688s1c1	CAAGGTGTTCTTTGACCTAAT
shIRF3-1	TRCN0000005919	NM_001571.1-1016s1c1	CCCTTCATTGTAGATCTGATT
shIRF3-2	TRCN0000005921	NM_001571.1-265s1c1	GCCAACCTGGAAGAGGAATTT
shcREL-1	TRCN0000039983	NM_002908.1-2071s1c1	CCACCTATATAGATGCAGCAT
shcREL-2	TRCN0000039986	NM_002908.1-981s1c1	CCAGGAAGTTAGTGAATCTAT
shcREL-3	TRCN0000010421	NM_002908.x-1875s1c1	CTTCAGTTGTGCAGATAACAG
shSurvivin	TRCT0000023441	NM_001168.1-214s1c1	CCAGTGTTTCTTCTGCTTCAA
shGFP	TRCN0000072181	clonetechGfp_437s1c1	ACAACAGCCACAACGTCTATA

Figure S1

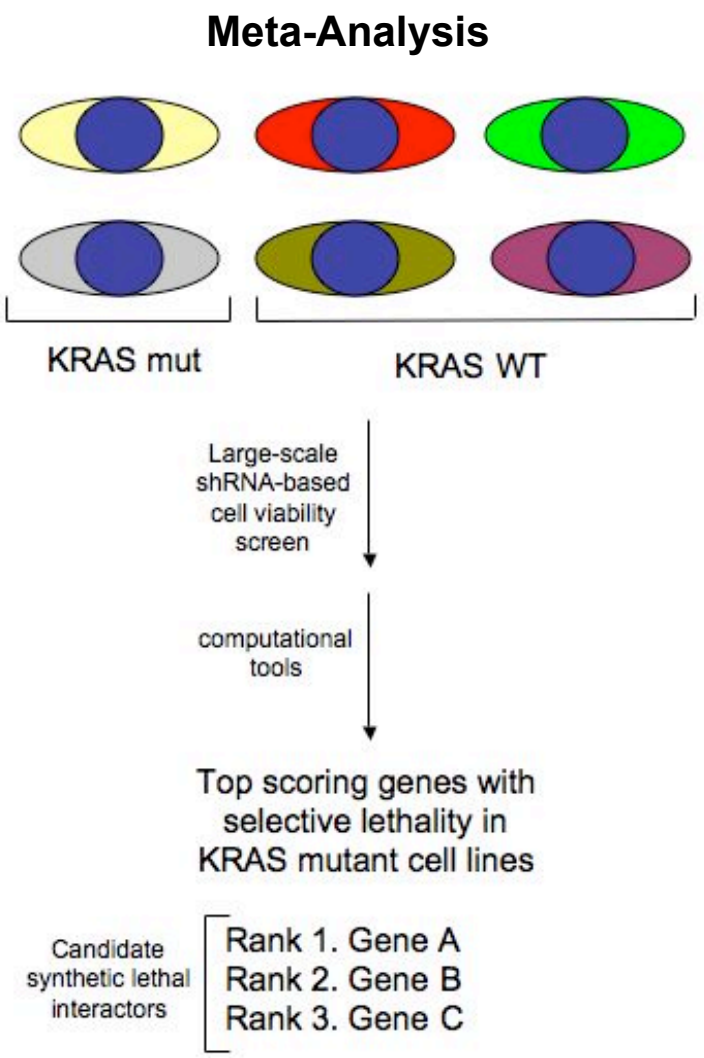
Meta-Analysis
KRAS mut
KRAS WT
Large-scale shRNA-based cell viability screen
computational tools
Top scoring genes with selective lethality in KRAS mutant cell lines
Candidate synthetic lethal interactors
Rank 1. Gene A
Rank 2. Gene B
Rank 3. Gene C

Figure S2

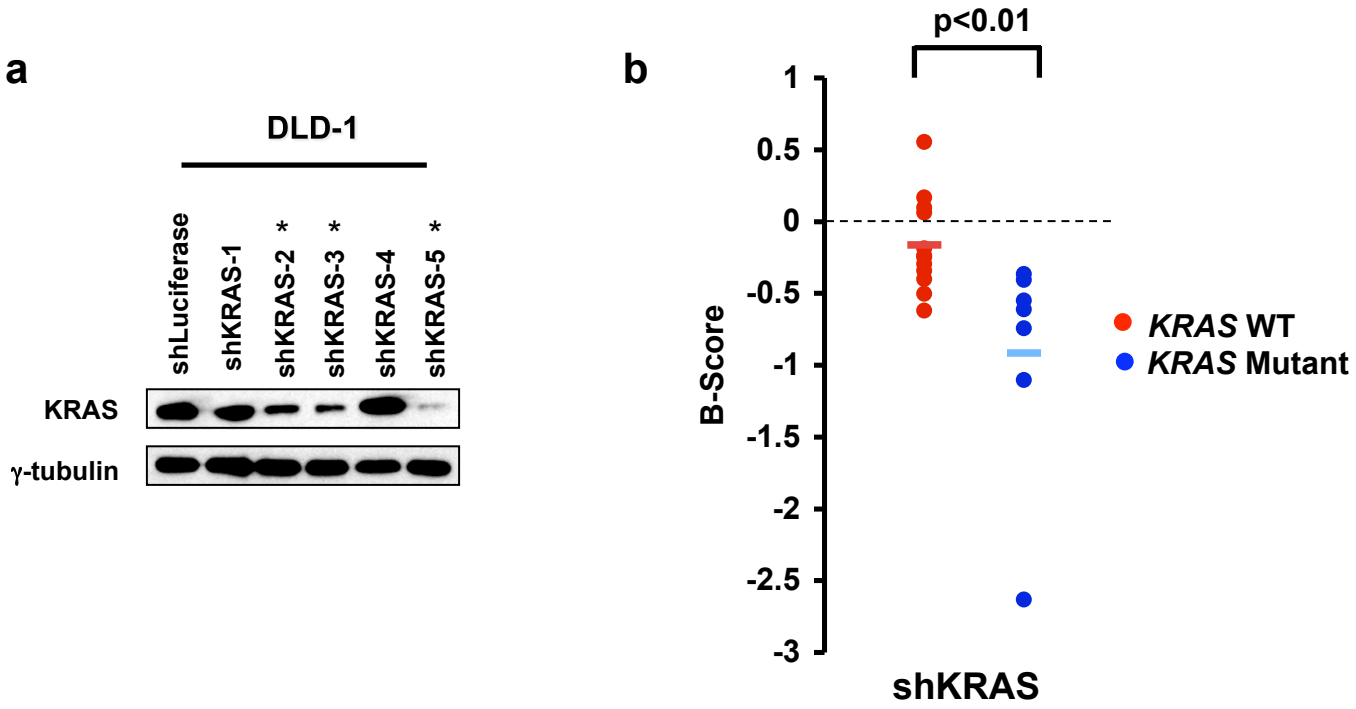
a
DLD-1
shLuciferase
shKRAS-1
shKRAS-2 *
shKRAS-3 *
shKRAS-4
shKRAS-5 *
KRAS
γ-tubulin
b
p<0.01
B-Score
1
0.5
0
-0.5
-1
-1.5
-2
-2.5
-3
shKRAS
KRAS WT
KRAS Mutant

Figure S3

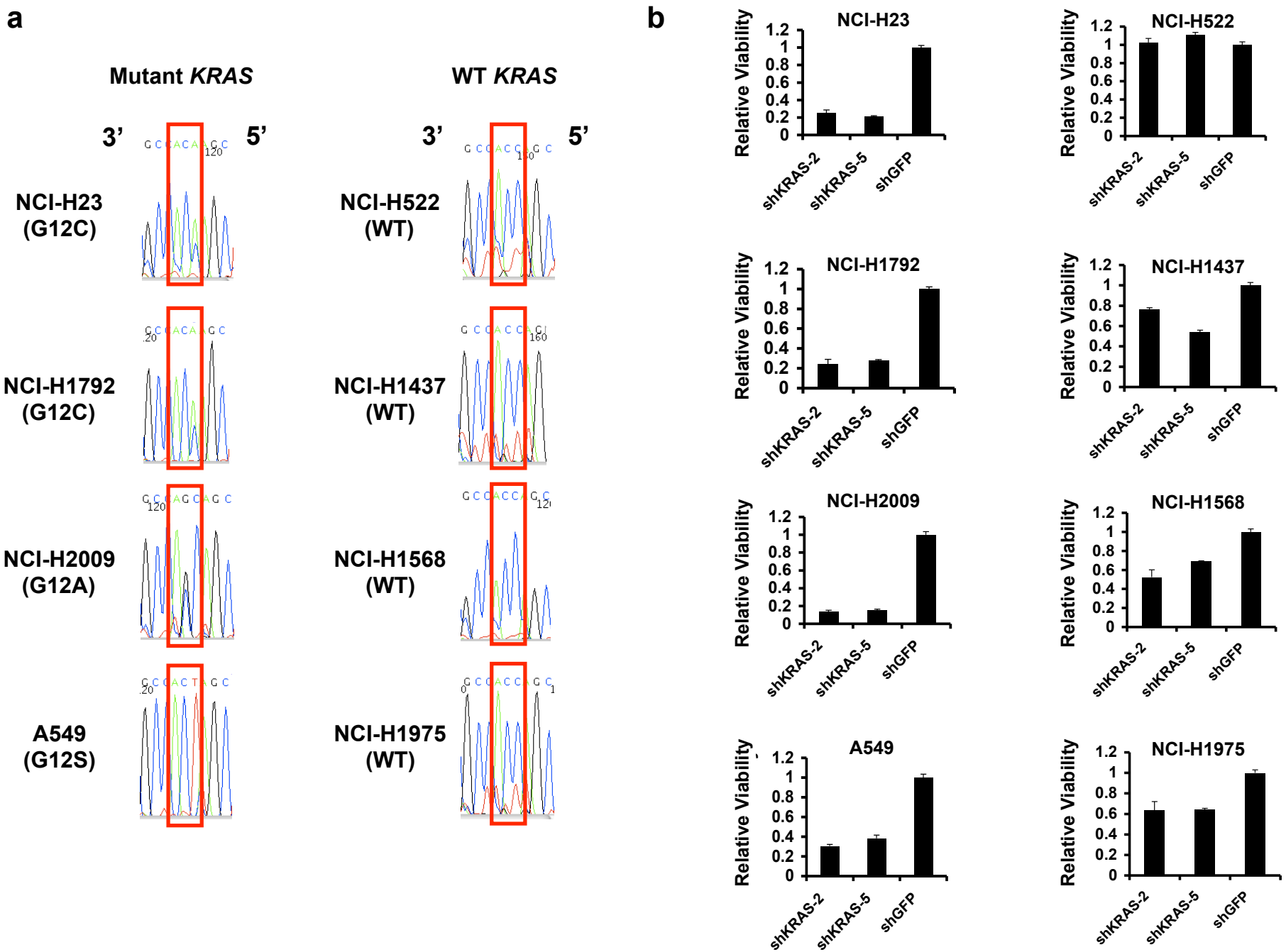
a
Mutant KRAS
WT KRAS
3'
5'
NCI-H23 (G12C)
NCI-H1792 (G12C)
NCI-H2009 (G12A)
A549 (G12S)
NCI-H522 (WT)
NCI-H1437 (WT)
NCI-H1568 (WT)
NCI-H1975 (WT)
b
Mutant KRAS
WT KRAS
Relative Viability
NCI-H23
NCI-H522
NCI-H1792
NCI-H1437
NCI-H2009
NCI-H1568
A549
NCI-H1975
shKRAS-2
shKRAS-5
shGFP

Figure S4

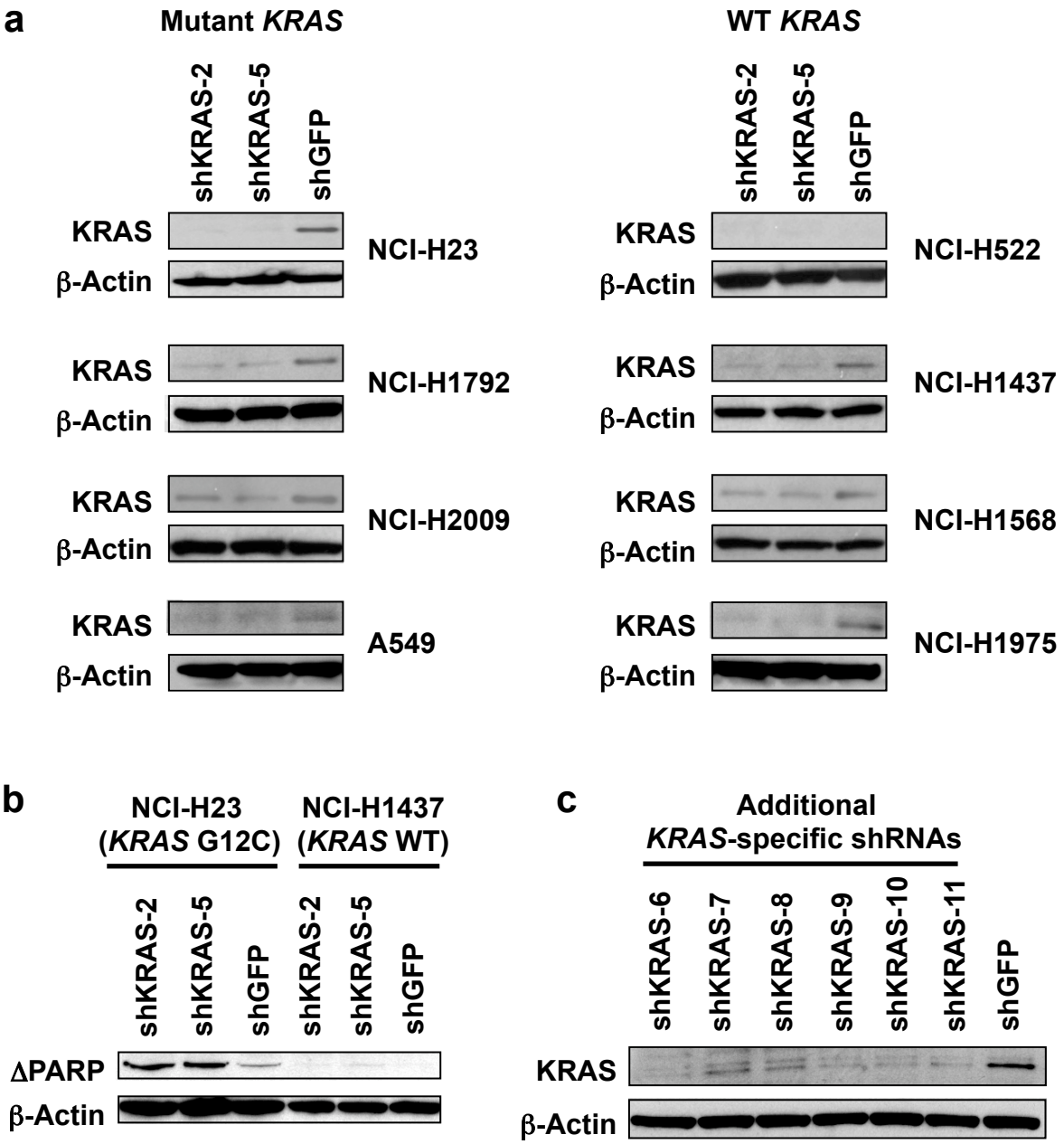
a
Mutant KRAS
WT KRAS
shKRAS-2
shKRAS-5
shGFP
KRAS
β-Actin
NCI-H23
NCI-H1792
NCI-H2009
A549
NCI-H522
NCI-H1437
NCI-H1568
NCI-H1975
b
NCI-H23
(KRAS G12C)
NCI-H1437
(KRAS WT)
ΔPARP
c
Additional
KRAS-specific shRNAs
shKRAS-6
shKRAS-7
shKRAS-8
shKRAS-9
shKRAS-10
shKRAS-11

Figure S5

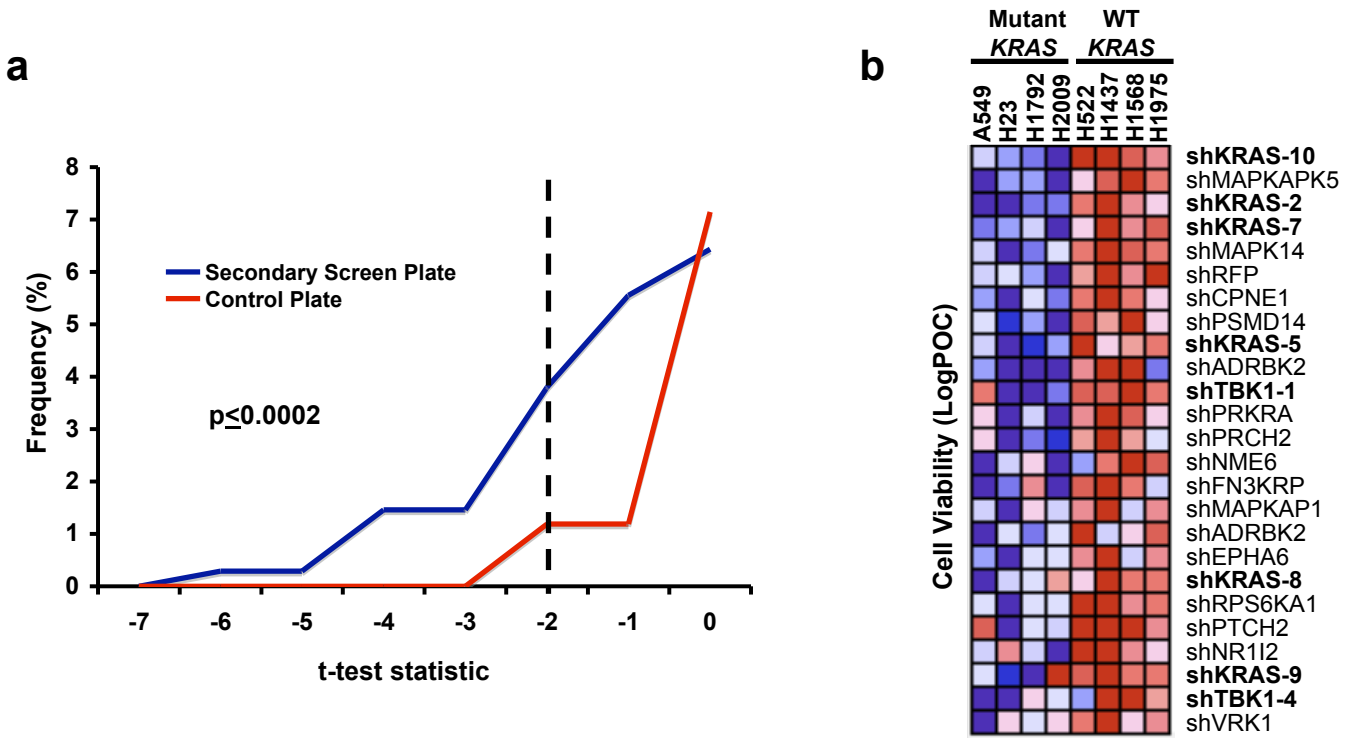
a
Frequency (%)
8
7
6
5
4
3
2
1
0
Secondary Screen Plate
Control Plate
p≤0.0002
-7
-6
-5
-4
-3
-2
-1
0
t-test statistic
b
Mutant KRAS
WT KRAS
A549
H23
H1792
H2009
H522
H1437
H1568
H1975
Cell Viability (LogPOC)
shKRAS-10
shMAPKAPK5
shKRAS-2
shKRAS-7
shMAPK14
shRFP
shCPNE1
shPSMD14
shKRAS-5
shADRBK2
shTBK1-1
shPRKRA
shPRCH2
shNME6
shFN3KRP
shMAPKAP1
shADRBK2
shEPHA6
shKRAS-8
shRPS6KA1
shPTCH2
shNR1I2
shKRAS-9
shTBK1-4
shVRK1

Figure S6

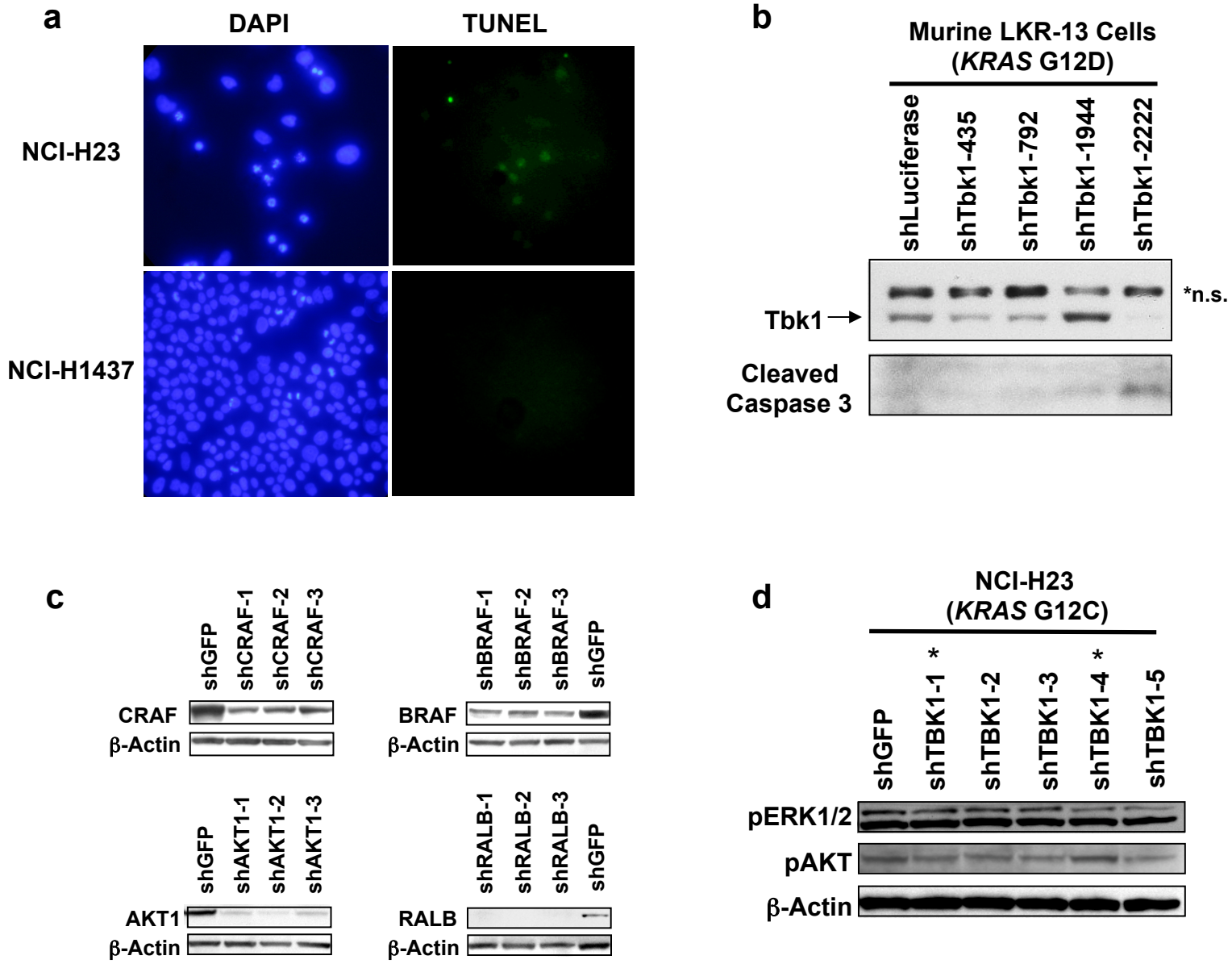
a
DAPI
TUNEL
NCI-H23
NCI-H1437
b
Murine LKR-13 Cells
(KRAS G12D)
shLuciferase
shTbk1-435
shTbk1-792
shTbk1-1944
shTbk1-2222
Tbk1
*n.s.
Cleaved
Caspase 3
c
shGFP
shCRAF-1
shCRAF-2
shCRAF-3
CRAF
β-Actin
shBRAF-1
shBRAF-2
shBRAF-3
shGFP
BRAF
β-Actin
shGFP
shAKT1-1
shAKT1-2
shAKT1-3
AKT1
β-Actin
shRALB-1
shRALB-2
shRALB-3
shGFP
RALB
β-Actin
d
NCI-H23
(KRAS G12C)
shGFP
shTBK1-1 *
shTBK1-2
shTBK1-3
shTBK1-4 *
shTBK1-5
pERK1/2
pAKT
β-Actin

Figure S7

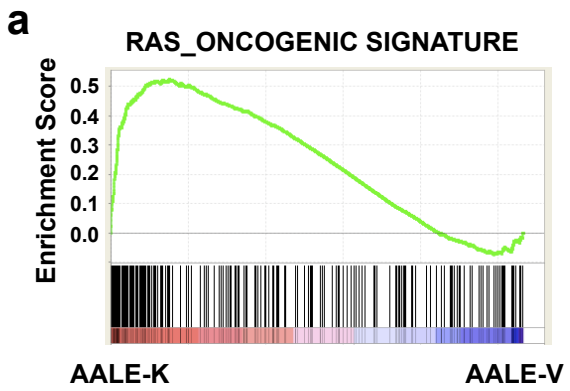

Upregulated in AALE-K

RANK	NAME	NES	FDR
1	**RAS_ONCOGENIC_SIGNATURE**	2.18	<0.001
2	HBX_HCC_UP	2.12	0.001
3	**HINATA_NFKB_UP**	2.08	0.002
4	**IKKE_NFKB_SUBSET**	1.97	0.039
5	DAC_CGI_BLADDER_UP	1.94	0.039
6	HSA00240_PYRIMIDINE_METABOLISM	1.94	0.035
7	SERUM_FIBROBLAST_CORE_UP	1.93	0.038
8	HBX_NL_UP	1.90	0.051
9	ADIPOCYTE_BRCA_UP	1.90	0.046
10	DORSEY_DOXYCYCLINE_UP	1.83	0.112
11	**TNFA_NFKB_DEP_UP**	1.80	0.159

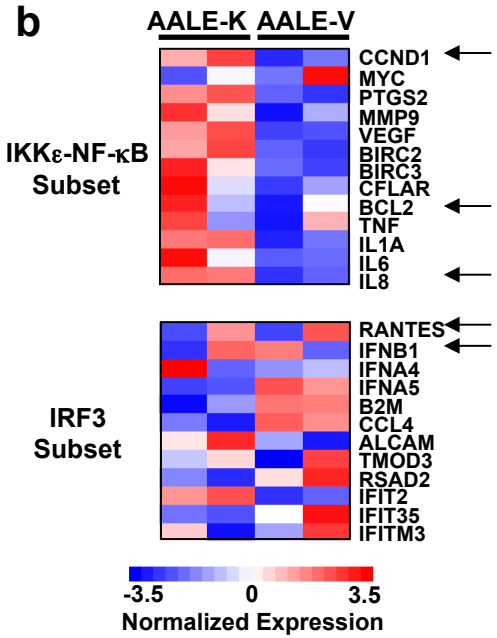

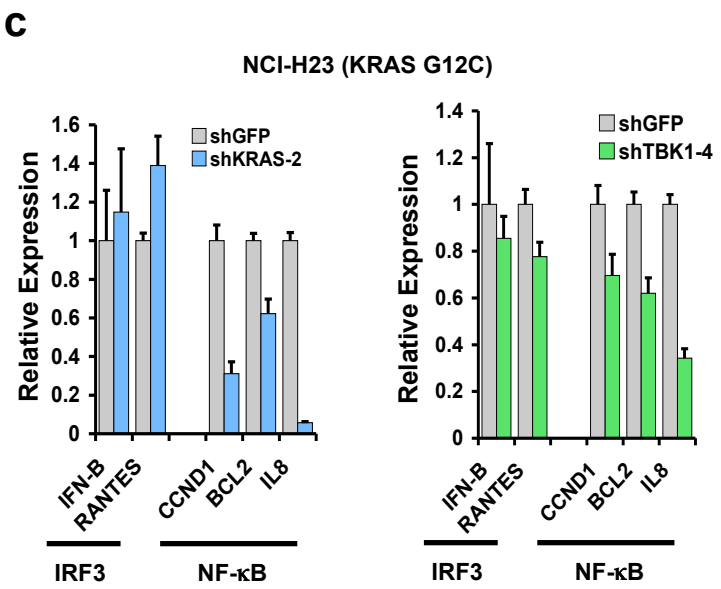

Figure S8

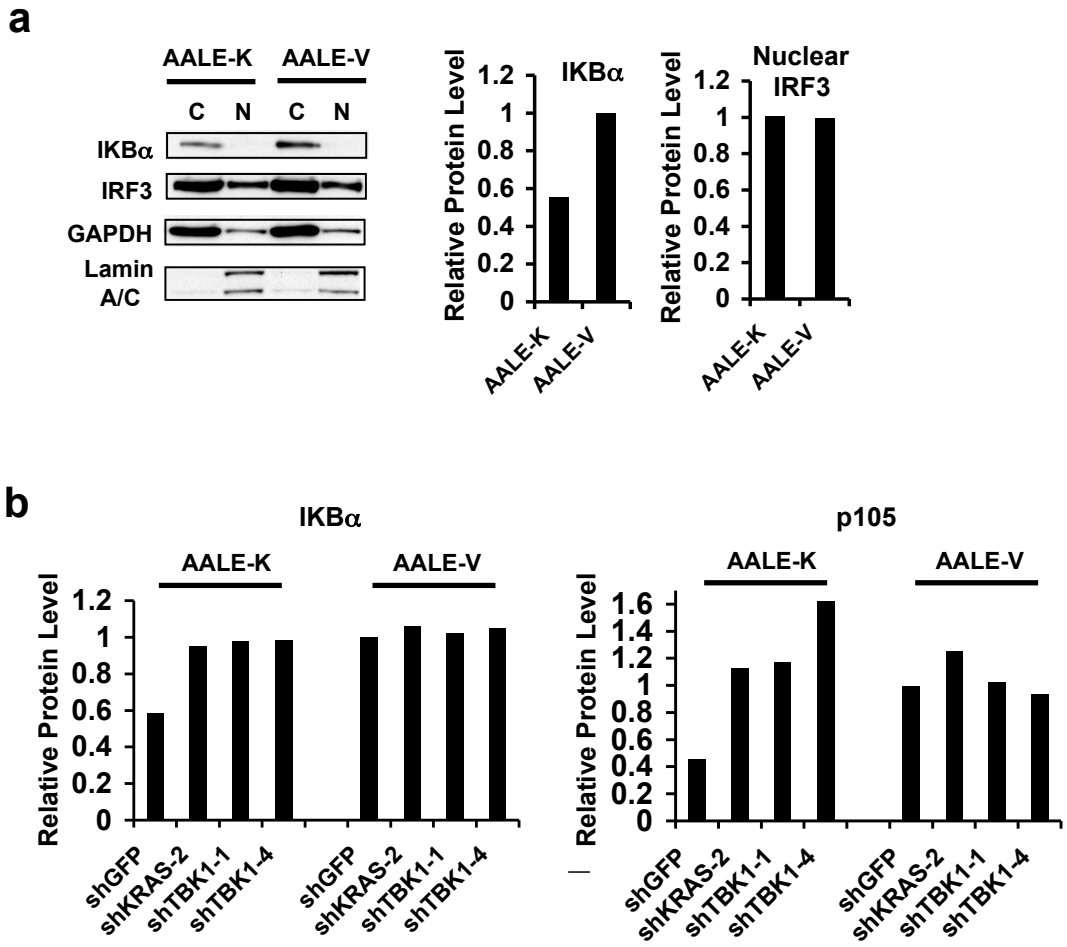
a
AALE-K
AALE-V
C
N
C
N
IKBα
IRF3
GAPDH
Lamin A/C
Relative Protein Level
IKBα
Nuclear IRF3
AALE-K
AALE-V
b
IKBα
p105
shGFP
shKRAS-2
shTBK1-1
shTBK1-4

Figure S9

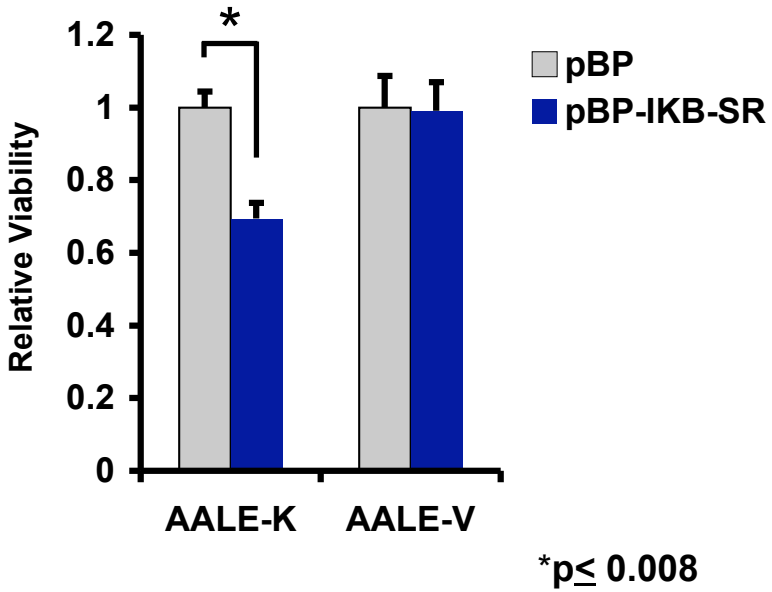
*
1.2
1
0.8
0.6
0.4
0.2
0
Relative Viability
AALE-K
AALE-V
pBP
pBP-IKB-SR
*p≤ 0.008

Figure S10

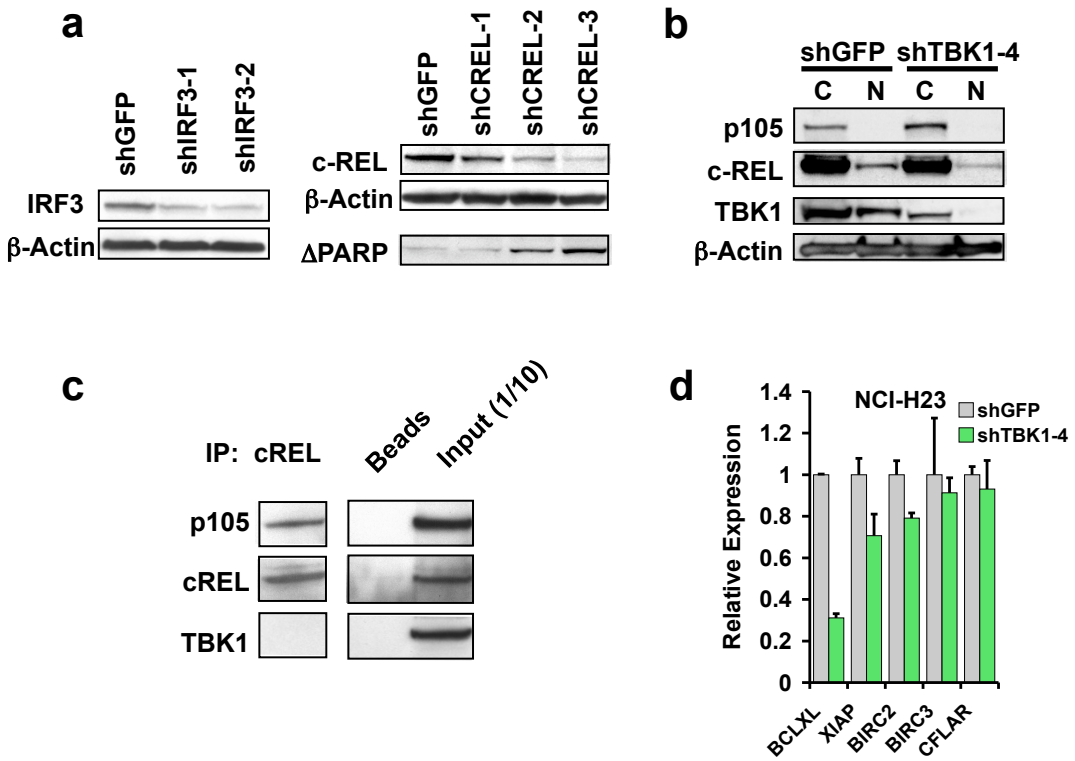
a
shGFP
shIRF3-1
shIRF3-2
IRF3
β-Actin
shGFP
shCREL-1
shCREL-2
shCREL-3
c-REL
β-Actin
ΔPARP
b
shGFP
shTBK1-4
C
N
C
N
p105
c-REL
TBK1
β-Actin
c
IP: cREL
Beads
Input (1/10)
p105
cREL
TBK1
d
NCI-H23
shGFP
shTBK1-4
Relative Expression
1.4
1.2
1
0.8
0.6
0.4
0.2
0
BCLXL
XIAP
BIRC2
BIRC3
CFLAR

Figure S11

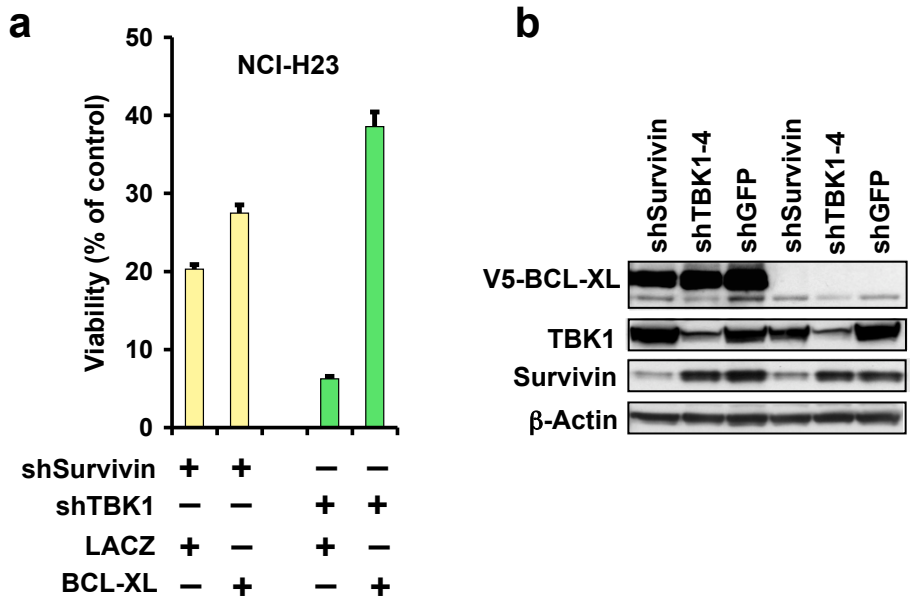
a
NCI-H23
Viability (% of control)
50
40
30
20
10
0
shSurvivin + + – –
shTBK1 – – + +
LACZ + – + –
BCL-XL – + – +
b
shSurvivin
shTBK1-4
shGFP
shSurvivin
shTBK1-4
shGFP
V5-BCL-XL
TBK1
Survivin
β-Actin